



Alternative Biosynthetic Starter Units Enhance the Structural Diversity of Cyanobacterial Lipopeptides

Jan Mareš,^{a,b,c} Jan Hájek,^{b,c} Petra Urajová,^b Andreja Kust,^{a,b,c} Jouni Jokela,^d Kumar Saurav,^b Tomáš Galica,^{b,c} Kateřina Čapková,^a Antti Mattila,^d Esa Haapaniemi,^{e,f} Perttu Permi,^e Ivar Mysterud,^g Olav M. Skulberg,^h Jan Karlsen,ⁱ David P. Fewer,^d Kaarina Sivonen,^d Hanne Hjorth Tønnesen,ⁱ Pavel Hrouzek^{b,c}

^aThe Czech Academy of Sciences, Biology Centre, Institute of Hydrobiology, České Budějovice, Czech Republic

^bThe Czech Academy of Sciences, Institute of Microbiology, Center Algatech, Třeboň, Czech Republic

^cUniversity of South Bohemia, Faculty of Science, České Budějovice, Czech Republic

^dDepartment of Microbiology, Viikki Biocenter, University of Helsinki, Helsinki, Finland

^eDepartment of Chemistry, University of Jyväskylä, Jyväskylä, Finland

^fDepartment of Biological and Environmental Science, Nanoscience Center, University of Jyväskylä, Jyväskylä, Finland

^gDepartment of Biosciences, University of Oslo, Oslo, Norway

^hNorwegian Institute for Water Research (NIVA), Oslo, Norway

ⁱSchool of Pharmacy, University of Oslo, Oslo, Norway

ABSTRACT Puwainaphycins (PUWs) and minutissamides (MINs) are structurally analogous cyclic lipopeptides possessing cytotoxic activity. Both types of compound exhibit high structural variability, particularly in the fatty acid (FA) moiety. Although a biosynthetic gene cluster responsible for synthesis of several PUW variants has been proposed in a cyanobacterial strain, the genetic background for MINs remains unexplored. Herein, we report PUW/MIN biosynthetic gene clusters and structural variants from six cyanobacterial strains. Comparison of biosynthetic gene clusters indicates a common origin of the PUW/MIN hybrid nonribosomal peptide synthetase and polyketide synthase. Surprisingly, the biosynthetic gene clusters encode two alternative biosynthetic starter modules, and analysis of structural variants suggests that initiation by each of the starter modules results in lipopeptides of differing lengths and FA substitutions. Among additional modifications of the FA chain, chlorination of minutissamide D was explained by the presence of a putative halogenase gene in the PUW/MIN gene cluster of *Anabaena minutissima* strain UTEX B 1613. We detected PUW variants bearing an acetyl substitution in *Symplocastrum muelleri* strain NIVA-CYA 644, consistent with an *O*-acetyltransferase gene in its biosynthetic gene cluster. The major lipopeptide variants did not exhibit any significant antibacterial activity, and only the PUW F variant was moderately active against yeast, consistent with previously published data suggesting that PUWs/MINs interact preferentially with eukaryotic plasma membranes.

IMPORTANCE Herein, we deciphered the most important biosynthetic traits of a prominent group of bioactive lipopeptides. We reveal evidence for initiation of biosynthesis by two alternative starter units hardwired directly in the same gene cluster, eventually resulting in the production of a remarkable range of lipopeptide variants. We identified several unusual tailoring genes potentially involved in modifying the fatty acid chain. Careful characterization of these biosynthetic gene clusters and their diverse products could provide important insight into lipopeptide biosynthesis in prokaryotes. Some of the variants identified exhibit cytotoxic and antifungal properties, and some are associated with a toxigenic biofilm-forming strain. The findings may prove valuable to researchers in the fields of natural product discovery and toxicology.

KEYWORDS biosynthesis, cyanobacteria, fatty acyl-AMP ligase, lipopeptides, nonribosomal peptide synthetase

Citation Mareš J, Hájek J, Urajová P, Kust A, Jokela J, Saurav K, Galica T, Čapková K, Mattila A, Haapaniemi E, Permi P, Mysterud I, Skulberg OM, Karlsen J, Fewer DP, Sivonen K, Tønnesen HH, Hrouzek P. 2019. Alternative biosynthetic starter units enhance the structural diversity of cyanobacterial lipopeptides. *Appl Environ Microbiol* 85:e02675-18. <https://doi.org/10.1128/AEM.02675-18>.

Editor Marie A. Elliot, McMaster University

Copyright © 2019 American Society for Microbiology. All Rights Reserved.

Address correspondence to Pavel Hrouzek, hrouzekp@gmail.com.

Received 5 November 2018

Accepted 28 November 2018

Accepted manuscript posted online 30 November 2018

Published 6 February 2019

Bacterial lipopeptides are a prominent group of secondary metabolites with pharmaceutical potential as antibacterial, antifungal, anticancer, and antiviral agents (1). Compounds like fengycin, the iturin family antibiotics, octapeptins, and daptomycin are important pharmaceutical leads, the latter of which is already in clinical use (1–3). Their biological activity is the result of an amphipathic molecular structure that allows micellar interaction within the cell membranes of target organisms (4).

Lipopeptides are widespread in cyanobacteria and possess cytotoxic and antifungal activities (5–8). Puwainaphycins (PUWs) and minutissamides (MINs) are lipopeptides featuring a β -amino fatty acid and a 10-membered peptide ring (5, 9–11). Both classes exhibit considerable structural variability in terms of length and functionalization of the fatty acyl (FA) side chain attached to the stable peptide core (10–14). Only minor discrepancies in the lengths and substitutions of the FA chain separate these two types of lipopeptides. A wide array of bioactivities has been reported for these compounds. PUW C is a cardioactive compound (15), as demonstrated by positive inotropic activity in mouse atria, while PUW F/G exhibit cytotoxicity against human cells *in vitro* through cell membrane permeabilization (5). MIN A to L exhibited antiproliferative effects over a range of concentrations when tested against human cancer cell lines, similarly to PUWs (10, 11). The overall structural similarity suggests that PUWs and MINs share a similar biosynthetic origin. However, the biosynthetic mechanisms generating the conspicuous chemical variability remain unknown.

PUWs are synthesized by a hybrid polyketide/nonribosomal peptide synthetase (PKS/NRPS) accompanied by tailoring enzymes (12). A characteristic feature of the PUW synthetase is the fatty acyl-AMP ligase (FAAL) starter unit (12). This enzyme specifically binds and adenylates FAs and passes the activated acyl-adenylate to a downstream phosphopantetheine arm of the PKS acyl carrier protein (ACP) for further processing (12). The whole process bears a resemblance to the biosynthesis of iturin family lipopeptides (16–19), as well as small lipopeptide-like cyanobacterial metabolites like hectochlorin (20), hapalosin (21), and jamaicamide (22), as discussed previously (23). Bacterial FAAL enzymes originate from basal cell metabolism and likely evolved from fatty acyl-coenzyme A (CoA) ligases (FACLs) following a specific insertion that hampered subsequent ligation to reduced CoA (CoASH) (24) or altered the catalytic conformation (25). FAAL enzymes play an important role in the assembly of other metabolites, including olefins (26) and unusual lipids (27), in addition to lipopeptide synthesis. The exact substrate-binding mechanism employed by FAALs was demonstrated experimentally in *Mycobacterium tuberculosis* using several homologous FAAL enzymes and FA substrates as models (28). The substrate specificity of these enzymes corresponds to the structure of the substrate-binding pocket (25, 28), although it overlaps among homologs.

Herein, we combined recently developed bioinformatics and high-performance liquid chromatography combined with high-resolution tandem mass spectrometry (HPLC–HRMS-MS) approaches (13, 23) to identify biosynthesis gene clusters for PUWs/MINs in five new cyanobacterial strains and characterized the chemical variability of their products. We discuss the specific structural properties of the lipopeptide variants identified and compare the predicted functions of synthetase enzymes.

RESULTS AND DISCUSSION

Structural variability versus common biosynthetic origin of PUWs and MINs. In the present study, we collected all known PUW/MIN producers (except for *Anabaena* sp. strain UIC10035). The strains, referred to herein as strains 1 to 6, were originally isolated from various soil habitats (Table 1). HPLC–HRMS-MS analysis detected multiple PUW and MIN variants in each of the strains studied (Fig. 1), ranging from 13 to 26 in strains 3 and 1, respectively (Table S1 in the supplemental material).

The MS-MS data acquired for crude extracts were used to create a molecular network (Fig. 2), analysis of which demonstrated that *Cylindrospermum* strains 1 to 3 and *Anabaena* strains 4 and 5 formed a single group with MIN A as the only variant common to all the strains (Fig. 2a). All major structural variants of these strains shared

TABLE 1 Strains analyzed for PUW/MIN production

Strain no. herein	Strain	Person who isolated strain	Date	Locality, habitat	Reference
1	<i>Cylindrospermum alatosporum</i> CCALA 988	A. Lukešová	1989	Canada, Manitoba, Riding Mountain National Park, soil	55
2	<i>Cylindrospermum moravicum</i> CCALA 993	A. Lukešová	2008	Czech Republic, South Moravia, Moravian Karst, Amaterska Cave, cave sediment	55
3	<i>Cylindrospermum alatosporum</i> CCALA 994	A. Lukešová	2011	Czech Republic, Moravian Karst, earthworms collected from soil above Amaterska Cave, earthworm casings	55
4	<i>Anabaena</i> sp. UHCC-0399	M. Wahlsten	N/A	Finland, Jurmo, Southwestern Archipelago National Park, copepods	56
5	<i>Anabaena minutissima</i> UTEX B1613	T. Kantz	1967	South Texas, USA, soil	57
6	<i>Symplocastrum muelleri</i> NIVA-CYA 644	O. M. Skulberg	2009	Norway, Møre og Romsdal county, Halså municipality, western slope of Slettjellet mountain in semiterrestrial alpine habitat, biofilm on turf in ombrotrophic blanket bog	40

the common peptide sequence FA¹-Val²-dehydroaminobutyric acid (Dhb)³-Asn⁴-Dhb⁵-Asn⁶-Ala⁷-Thr⁸-*N*-methyl-L-asparagine (NMeAsn)⁹-Pro¹⁰ (Fig. 3), described previously for PUW F and MIN A (5, 10). The pattern of variant production was almost identical in *Cylindrospermum* strains 2 and 3, which in addition to MIN A contained PUW F (Fig. 1, Table S1). In contrast, *Anabaena* strains 4 and 5 produced MIN C and D in addition to the major variant, MIN A (Fig. 1). The peptide core of the molecule was different in *Symplocastrum muelleri* strain 6 (Fig. 3), forming a separate group in the molecular network (Fig. 2b), with the general peptide sequence FA¹-Val²-Dhb³-Thr⁴-Thr/Val⁵-Gln⁶-Ala⁷-*O*-methyl-L-threonine (OMeThr)⁸-NMeAsn⁹-Pro¹⁰ (Fig. 3), identical to those of PUW A to D and MIN I, K, and L isolated previously from *Anabaena* sp. (9, 11).

The peptide cores of the variants included in the network differed to some degree, but most variation was detected in the FA moiety (Fig. 4) when crude extracts were analyzed for the presence of characteristic FA immonium fragments (13).

Accordingly, bioinformatic analysis identified putative PUW and MIN gene clusters in each of the five newly sequenced strains (Fig. 5, Table 2). Based on BLASTp, CDD, and AntiSMASH searches, these gene clusters exhibited synteny and functional homology with the previously characterized *puw* biosynthesis gene cluster in strain 1 (12) (Fig. 5). Therefore, our results strongly indicate a common biosynthetic origin of PUWs and MINs in cyanobacteria.

Variability in the peptide core. A common set of NRPS genes (*puwA* and *puwE* to *-H*) (Fig. 5) encoding a sequence of nine amino acid-incorporating modules (Fig. 6) was detected in all strains analyzed. Individual NRPS modules displayed variability in amino acid adenylation and tailoring domains that was generally congruent with the PUW/MIN peptide cores inferred using HPLC–HRMS–MS (Fig. 3). The two major types of peptide cores observed (represented by PUW A and PUW F, respectively) differed in the amino acids at positions 4 (Thr→Asn), 5 (Thr→Dhb), 6 (Gln→Asn), 7 (Ala→Gly), and 8 (Thr→OMe-Thr), as shown in Fig. 3 and Table S1. This was reflected in the predicted substrates of the corresponding adenylation domains (A domains) and by the presence of an *O*-methyltransferase domain in *puwH* of *S. muelleri* strain 6, which is responsible for the methoxylation of Thr⁸ (Fig. 6, Table S2). In contrast to the variability observed at the previously noted amino acid positions, the two positions adjacent to both sides of the modified fatty acid [NMeAsn⁹-Pro¹⁰-(FA¹-Val²-Dhb³)] are conserved in all known PUW/MIN variants described here and previously (5, 9, 13–15) (Fig. 3, Table S1). Accordingly, no functional variation in A domains corresponding to these positions was observed within the deduced *puwA*, *puwE*, and *puwF* proteins (Table S2). This is interesting because these four hydrophobic amino acids surround the FA moiety, which is likely responsible for the membrane disruption effect suggested previously (5). Thus, we hypothesize that such an arrangement could further support hydrophobic interactions with the lipid layer of the plasma membrane.

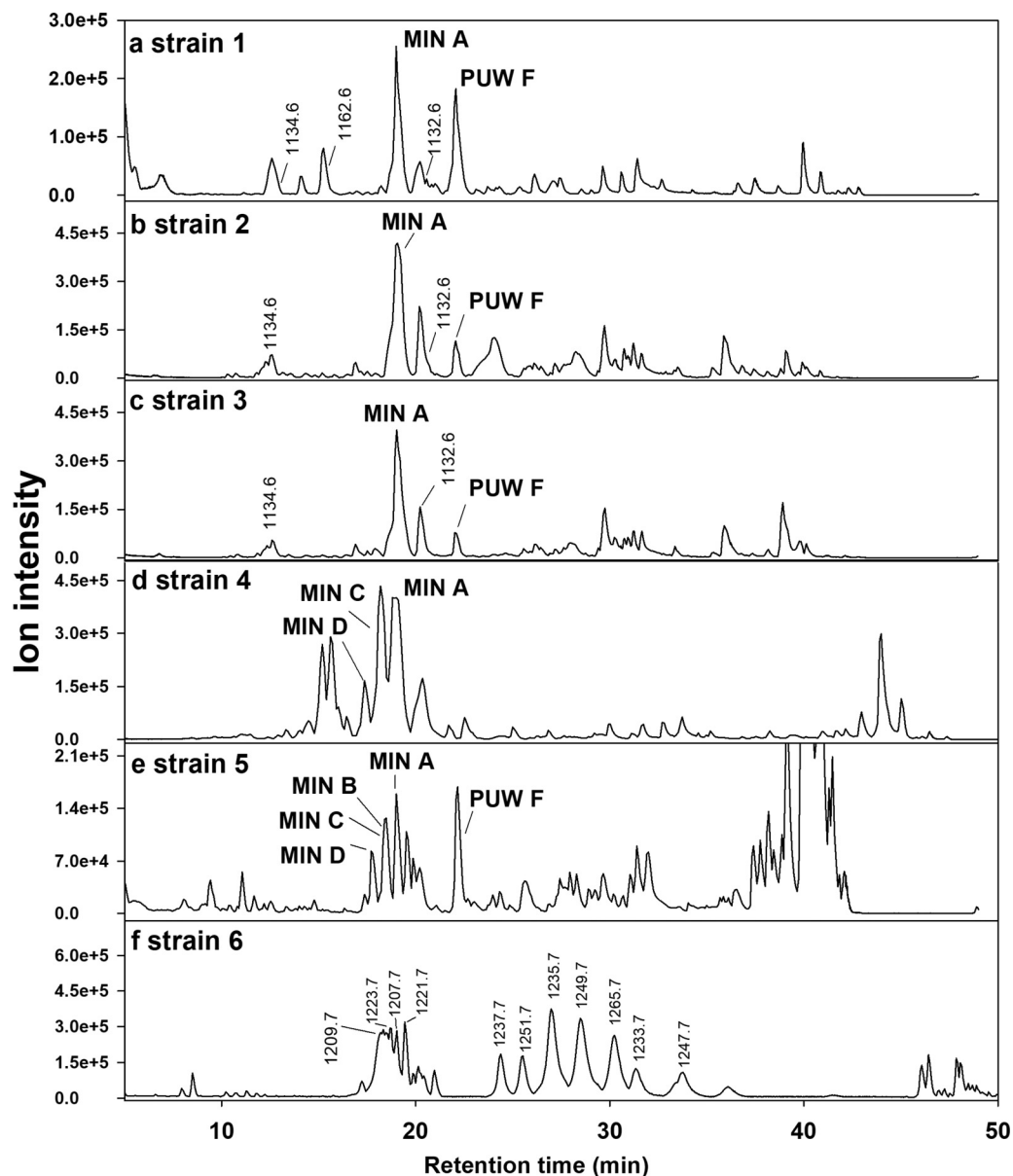


FIG 1 HPLC–HRMS–MS analysis of crude extracts from the strains investigated. Major puwainaphycin (PUW) and minutissamide (MIN) variants are highlighted. For variants without complete structural information, only m/z values are shown.

For some of the other positions, minor variants were observed involving substitution of amino acids similar in structure and hydrophobicity, including Asn-Gln at position 4, Thr-Val at position 5, Ala-Gly at position 7, and Thr-Ser at position 8 (Fig. 3, Table S1), indicative of probable substrate promiscuity in their respective adenylation domains (29). The A6 domains in strains 4 and 5 activated Ala as a major substrate and Gly to a lesser extent, even though *in silico* analysis predicted Gly as their main substrate (Table S2). In strain 6, Gly was incorporated, in agreement with the predicted substrate specificity. An epimerase domain was present in each of the sixth NRPS modules (i.e., C-A6-PCP) of the pathways (Fig. 6), indicating the probable formation of a D-amino acid enantiomer at position 7 of the peptide core. Indeed, the presence of D-Ala was previously confirmed in PUW F (5) and MIN A to H (10, 11), and D-Gly was identified in MIN I to L (10, 11). In two cases, the adenylation domains A3 (PuwF) and A6 (PuwG) are capable of incorporating significantly different amino acids, such as Asn⁴-Thr⁴ and Ala⁷-Ser⁷, respectively (Fig. 6). This degree of substrate promiscuity is relatively uncom-

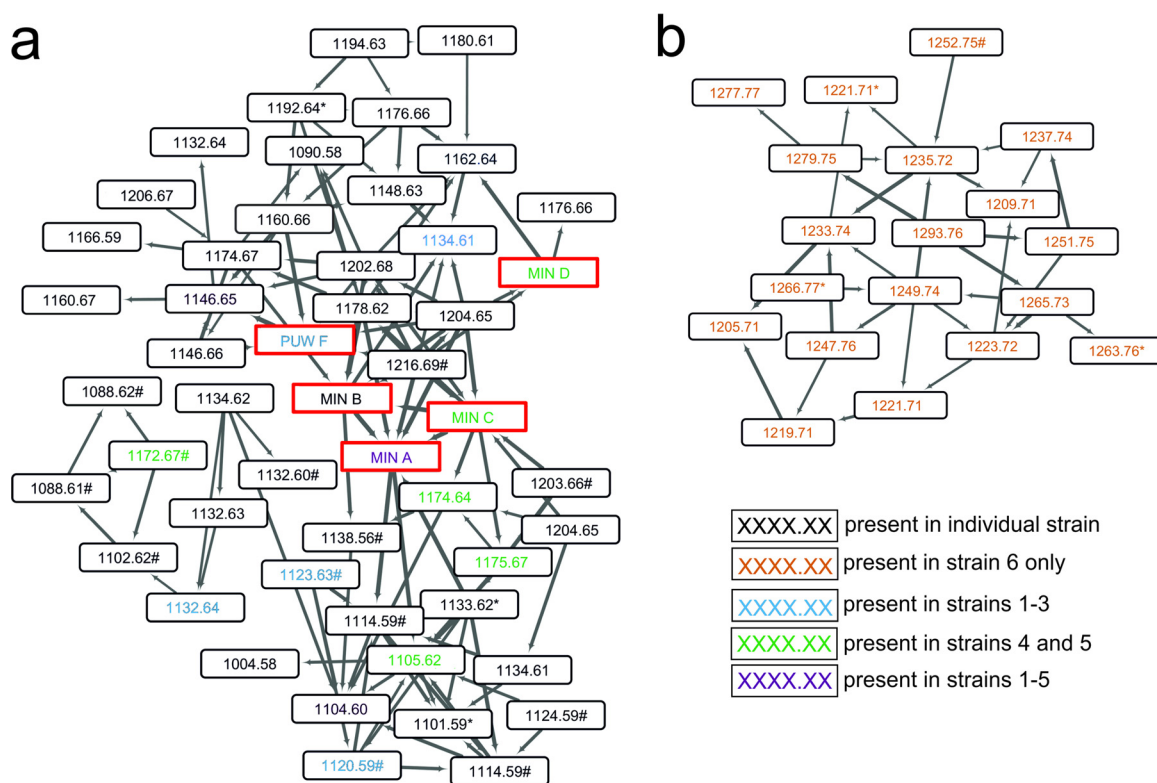
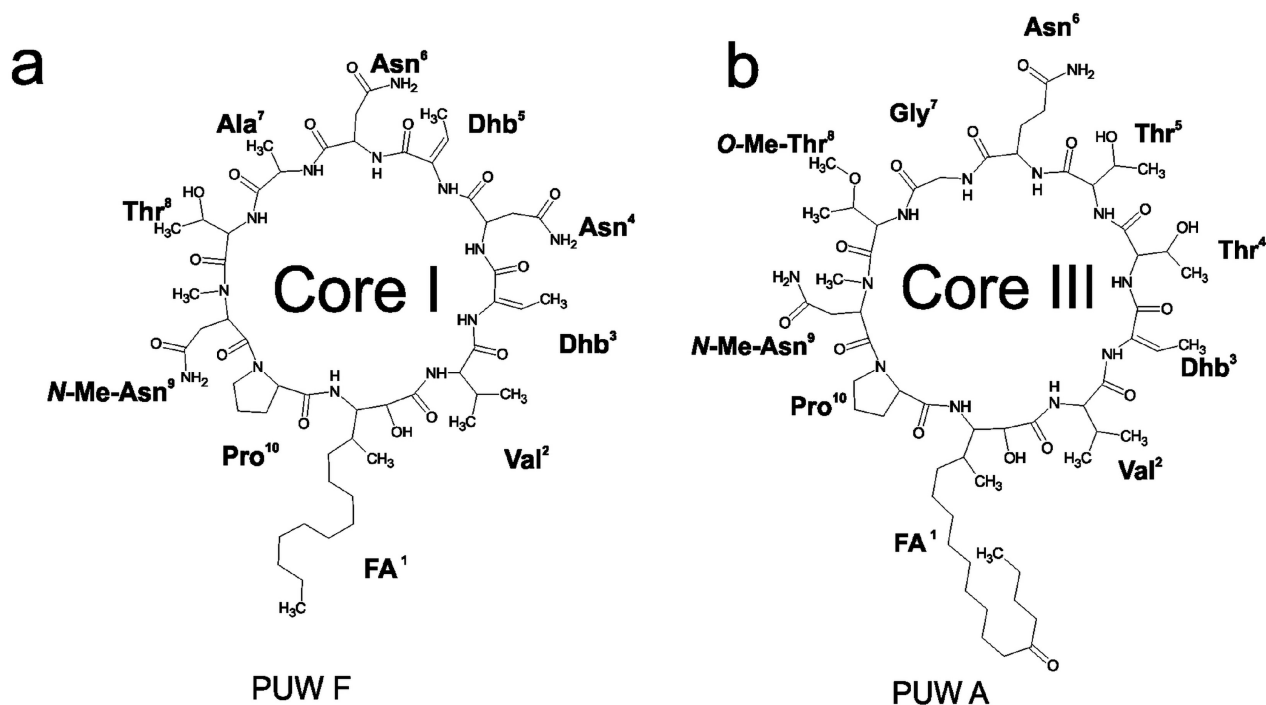


FIG 2 Molecular network created using the Global Natural Products Social Molecular Networking (GNPS) web platform. Two separate networks were obtained during GNPS analysis: a group containing *Cylindrospermum* strains 1 to 3 and *Anabaena* strains 4 and 5 (a), and a group containing only variants detected in *Symplocastrum muelleri* strain 6 (b). The separate groups differ mainly in the peptide core of the molecule. For variants without complete structural information, only *m/z* values are shown. *, compound present in trace amounts; #, compound for which MS-MS data failed to resolve the structural information.

mon. The activation of two divergent amino acids (Arg/Tyr) by a single adenylation domain, based on point mutations in just three codons, was previously demonstrated in the anabaenopeptin synthetase from the cyanobacterium *Planktothrix agardhii* (30). The substrate exchange of Ala versus Ser was previously reported from fungal class IV adenylation-forming reductases that contain A domains homologous to those of NRPS enzymes (31).

The last synthetase enzyme in the pathway (PuwA) is equipped with a terminal thioesterase domain (Fig. 6), which presumably catalyzes cleavage of the final product and formation of the cycle via a peptide bond between the terminal prolyl and the β -amino group of the FA chain, as previously suggested (12).

Two hypothetical starter units and their substrate range. The biosynthesis of bacterial lipopeptides is typically commenced by FA-activating enzymes (16, 18). Initiation of the biosynthesis of PUW/MIN is performed by a FAAL enzyme (12) and allows a much broader array of activated substrates than the relatively conserved oligopeptide core (Fig. 4) (13). We identified three alternative arrangements of the putative FAAL starter units (Fig. 5 and 6), each corresponding to a different array of FA side chains detected by HPLC–HRMS-MS, which presumably reflects the range of FA substrates activated during their biosynthesis (Fig. 4). *Cylindrospermum* species strains 1 to 3 possess the type I putative starter unit consisting of a standalone FAAL enzyme, PuwC, and a separate ACP, PuwD (Fig. 5, Table 2). In contrast, the biosynthetic gene cluster of *S. muelleri* strain 6 contains the type II putative starter unit (PuwI) consisting of a FAAL fused to an ACP (Fig. 5, Table 2). *Anabaena* species strains 4 and 5 combine both type I and type II putative starter units in their biosynthetic gene clusters (Fig. 5, Table 2). Although the functions and substrate ranges of these hypothetical starter units require further confirmation by gene manipulation experiments, they are supported by the



C

	AA ₁	AA ₂	AA ₃	AA ₄	AA ₅	AA ₆	AA ₇	AA ₈	AA ₉	AA ₁₀	known compounds	variants found in strains 1-6
Core I	FA	Val	Dhb	Asn	Dhb	Asn	Ala	Thr	<i>N</i> -Me-Asn	Pro	MIN A, MIN B, MIN C, MIN D, PUW F	MIN A, MIN B, MIN C, MIN D, PUW F, Comp. 1,3,10,11,12,14,16,19,20,25,26,28,30,31,37,45,51
Core II	FA	Val	Dhb	Gln	Dhb	Asn	Ala	Thr	<i>N</i> -Me-Asn	Pro	PUW G	PUW G, Comp. 2,6,13,15,17,27,29,32
Core III	FA	Val	Dhb	Thr	Thr	Gln	Gly	<i>O</i> -Me-Thr	<i>N</i> -Me-Asn	Pro	PUW A, PUW C, PUW E, MIN I, MIN K	Comp. 38,46,50,52,53,56,58
Core IV	FA	Val	Dhb	Thr	Thr	Gln	Ala	<i>O</i> -Me-Thr	<i>N</i> -Me-Asn	Pro	MIN E, MIN G	Comp. 39,47,53,57,59
Core V	FA	Val	Dhb	Thr	Val	Gln	Gly	<i>O</i> -Me-Thr	<i>N</i> -Me-Asn	Pro	PUW B, PUW D, MIN L	Comp. 40,48,54,60
Core VI	FA	Val	Dhb	Thr	Val	Gln	Ala	<i>O</i> -Me-Thr	<i>N</i> -Me-Asn	Pro	MIN H	Comp. 41,49,55,61
Core VII	FA	Val	Dhb	Asn	Dhb	Asn	Gly	Thr	<i>N</i> -Me-Asn	Pro		Comp. 7,36,44
Core VIII	FA	Val	Dhb	Asn	Dhb	Asn	Ser	Thr	<i>N</i> -Me-Asn	Pro		Comp. 8,23,35
Core IX	FA	Val	Dhb	Asn	Dhb	Asn	Ala	Ser	<i>N</i> -Me-Asn	Pro		Comp. 9,18,24
Core X	FA	Val	Dhb	Thr	Dhb	Asn	Ala	Thr	<i>N</i> -Me-Asn	Pro		Comp. 5,34,43

FIG 3 Structural variability of the peptide cores of PUW/MIN variants. Examples of structural variants PUW F (a) and PUW A (b) with designated amino acid positions representing the two major peptide cores. (c) Table summarizing all types of the PUW/MIN peptide core found in known compounds reported in literature and compounds (Comp.) detected in studied strains. Columns shaded in gray highlight the conserved amino acid positions.

patterns of lipopeptide variants detected by HPLC–HRMS–MS (Fig. 4, Table S1). In *Cylindrospermum* strains 1 to 3, which exclusively contain the type I starter unit, the PUW/MIN products exhibited an almost-continuous FA distribution of between C₁₀ and C₁₅ (up to C₁₇ in negligible trace amounts) (Fig. 4). In *S. muelleri* strain 6, the presence of the type II loading module resulted in the production of PUW/MIN variants with discrete FA lengths of C₁₆ and C₁₈. Strains containing both type I and type II starter units (*Anabaena* strains 4 and 5) produced two sets of PUW/MIN products with no overlap (C₁₂ to C₁₄₋₁₅ for the type I pathway and C₁₆ for the type II pathway) but exhibited a slightly shifted length distribution (Fig. 4). Based on these results, it seems plausible that PuwC/-D and PuwI represent two alternative FAAL starter modules capable of initiating PUW/MIN biosynthesis (Fig. 5 and 6). An analogous situation was previously described for the alternative NRPS starter modules in the anabaenopeptin synthetase (32).

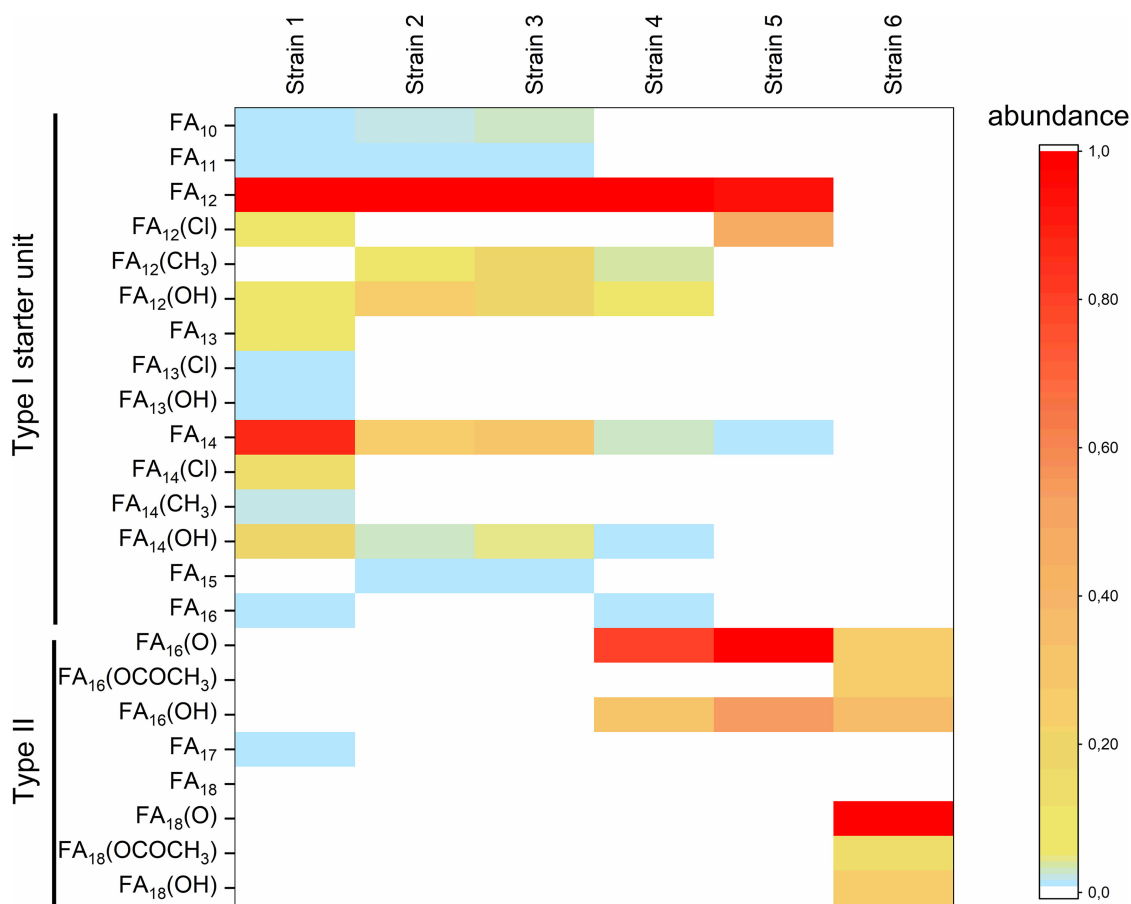


FIG 4 Structural variability of the FA moiety of PUW/MIN variants. The relative proportions of variants with differences in FA lengths and substitutions are depicted using a color scale. For comparison, the peak area of a given variant was normalized against the peak area of the major variant present in the strain (MIN A for strains 1 to 5 and *m/z* 1,235.7 for strain 6).

In the FA residue of the lipopeptide, proximal carbons in the linear aliphatic chain are incorporated into the nascent product by PKS enzymes (12). The PKS domains of PuwB and PuwE (Fig. 6, Table 2) catalyze two elongation steps. Therefore, the fatty acid is expected to be extended by four carbons. The substrate length specificities of the

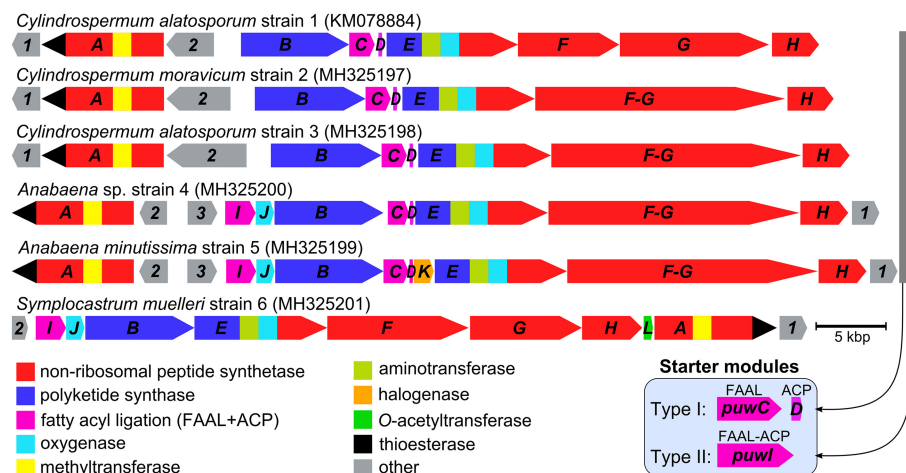


FIG 5 Structures of the *puw* gene cluster in the six cyanobacterial strains investigated. Gene arrangement and functional annotation of *puwA* to *-L* genes and selected PKS/NRPS tailoring domains are indicated by colored arrows. The distribution of the two types of putative starter modules (shaded boxes) observed is indicated by bars.

TABLE 2 Deduced proteins encoded by the *puw* gene cluster in six cyanobacterial strains, including length and functional annotation^c

Protein	Length (aa) in strain no.:						Predicted function(s) ^a
	1	2	3	4	5	6	
ORF1	659	664	664	643	643	647	ABC transporter
PuwA	2,870	2,870	2,870	2,854	2,854	2,866	NRPS
ORF2	1,116	1,499	1,875	643	670	376	Patatin-like phospholipase
ORF3				696	696		Dynamin family protein
PuwI				709	702	711	FAAL, ACP
PuwJ				427	427	529	Cytochrome-like protein
PuwB	2,534	2,592	2,592	2,549	2,537	2,555	Hybrid PKS/NRPS, aminotransferase, oxygenase
PuwC	597	590	590	597	589		FAAL
PuwD	101	104	96	93	92		ACP
PuwK					465		Halogenase
PuwE	3,077	3,121	3,121	3,099	3,112	3,113	NRPS
PuwF	2,370	5,851 ^b	5,851 ^b	5,877 ^b	5,871 ^b	3,310	NRPS
PuwG	3,492					2,620	NRPS
PuwH	1,102	1,081	1,102	1,121	1,121	1,408	NRPS
PuwL						217	O-Acetyltransferase

^aACP, acyl carrier protein; FAAL, fatty acyl-AMP ligase; PKS, polyketide synthase; NRPS, nonribosomal peptide synthetase.

^bThe proteins PuwF and PuwG are encoded in a single ORF in this strain.

^cThe empty fields in the table indicate the absence of a particular protein.

FAAL enzymes in *Mycobacterium tuberculosis* were recently shown to be determined by the size and position of specific amino acid residues protruding into the FA-binding pocket (28). Experimental replacement of Gly or Ile by a larger Trp residue in the upper and middle parts of the pocket blocked the binding of the original C₁₂ substrate, but shorter chains (C₂ or C₁₀, respectively) were still activated (28). Experimental data on FAAL substrate specificity in cyanobacteria are currently lacking. Alignment of amino acid residues from all putative PuwC and PuwI proteins demonstrates overall homology (Fig. S2a), including the positions corresponding to the FA-binding pocket, as previously shown in *Mycobacterium* (Fig. S2b) (28). Experimental evidence, such as *in vitro*

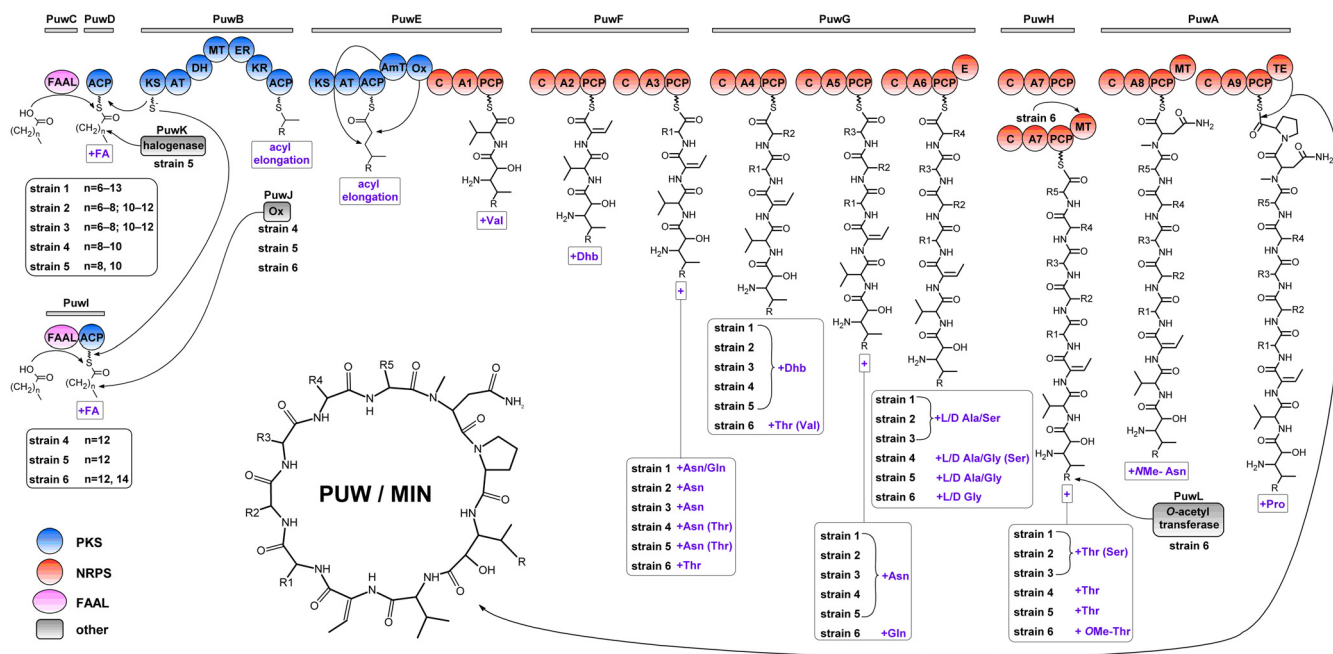


FIG 6 Schematic view of the proposed biosynthesis assembly line of puwainaphycins and minutissamides. Variable amino acid positions and the ranges of fatty acyl lengths incorporated by the two putative alternative starter units are listed for individual strains. A, adenylation domain; ACP, acyl carrier protein; AmT, aminotransferase; AT, acyltransferase; C, condensation domain; DH, dehydratase; E, epimerase; ER, enoylreductase; FAAL, fatty acyl-AMP ligase; MT, methyltransferase; NRPS, nonribosomal peptide synthetase; KR, ketoreductase; KS, ketosynthetase; Ox, monooxygenase; PCP, peptidyl carrier protein; PKS, polyketide synthetase; TE, thioesterase.

activity assays and crystallization of protein-ligand complexes, is required to explain the varying substrate specificities of PuwC versus those of PuwL. Also, we cannot exclude the possibility that the FA substrate length range is partially determined by the pool of free FAs available to the FAAL enzyme. Indeed, this possibility is supported by observations of *Cylindrospermum* strains 1 to 3, which share highly conserved PuwC proteins (Fig. S2a) with identical residues in the predicted FA-binding pockets (Fig. S2b) but display slightly different ranges and ratios of incorporated FAs in the PUW/MIN variants produced (Fig. 1 and 4).

FA tailoring reactions: oxidation, halogenation, and acetylation. Intriguingly, all products originating from biosynthesis initiated by the type II starter unit (variants with C_{16} and C_{18} FA tails in *Anabaena* strains 4 and 5 and *S. muelleri* strain 6) include the substitution of a hydroxy or oxo moiety (Fig. 6). For minutissamides C and D, this substitution takes place on the third carbon from the FA terminus (C_{14}), as described previously (10), and this position was confirmed by nuclear magnetic resonance (NMR) in variants produced by *Anabaena* sp. strain 4 in our study (Table S3, Fig. S3 to S6). In agreement with these hydroxy and oxo substitutions, the respective gene clusters each encode PuwJ, a putative cytochrome P450-like oxidase (Table 2), immediately downstream from the gene encoding the type II starter module. We therefore hypothesize that the PuwJ enzyme is responsible for hydroxylation of FA residues activated by PuwL (Fig. 6). However, the formation of the keto variant remains unexplained by our data.

Another gene, *puwK*, encoding a putative halogenase, was associated with the type II starter module in *Anabaena* sp. strain 5 (Table 2). Although no conserved enzymatic domain was detected in the deduced protein, it shares similarity with proteins postulated to be involved in the halogenation of cyanobacterial chlorinated acyl amides known as columbamides (33) and *N*-oxygenases similar to the *p*-aminobenzoate *N*-oxygenase AurF (34–36). The possible functional designation of this enzyme as a halogenase is further supported by the fact that the ω -chlorinated product MIN B, originally described in *Anabaena* sp. strain 5 (10), was also detected in this study (Table S1) as one of the major variants, while no MIN B or any other chlorinated PUW/MIN products were detected in *Anabaena* sp. strain 4 (Fig. 1). *Anabaena* species strains 4 and 5 share identical organization across the entire gene cluster, and the lack of the putative halogenase gene *puwK* is the only difference between these two clusters in terms of the presence of genes (Fig. 5).

In *Cylindrospermum* species strains 1 to 3, which exclusively possess the type I starter unit, the presence of minor amounts of hydroxylated and chlorinated variants (Fig. 4) suggests the involvement of another biosynthetic mechanism unexplained by the current data. This ambiguity warrants experimental research, such as gene knockout experiments, to confirm the proposed functions of *puwJ* and *puwK*.

Finally, the gene cluster identified in *S. muelleri* strain 6 was the only one containing gene *puwL*. The deduced product of this gene shares 53.4% similarity with the *O*-acetyltransferase McyL (Table 2), which is involved in acetylation of the aliphatic chain of microcystin in cyanobacteria (37). Additionally, this gene is similar to those encoding chloramphenicol and streptogramin A *O*-acetyltransferases that serve as antibiotic resistance agents in various bacteria (38). The functional annotation of PuwL as a putative *O*-acetyltransferase is consistent with the detection of *O*-acetylated lipopeptide variants in *S. muelleri* strain 6 (Table 3, Fig. 7). Five PUW variants (m/z 1,265.7338, 1,279.7496, 1,277.7695, 1,291.7870, and 1,293.7654) that yield high-energy fragments proving the presence of an acetyl group bonded to the FA moiety have been detected. In the m/z 1,279.8 and 1,293.8 peaks, the high-energy-fragment ion at m/z 312 corresponds to the FA immonium ion bearing an acetyl group, and the fragment ion at m/z 439 corresponds to the prolyl-FA-acetyl fragment. The subsequent loss of an acetyl group resulted in the presence of ions at m/z 252 and 379, respectively (Table 3, Fig. 7). Similarly, analysis of the m/z 1,265.7 peak revealed analogous fragments at m/z 284/411 and 351/224 (Table 3).

TABLE 3 Fragmentation and amino acid composition of PUW variants from *Symplocastrum muelleri* strain 6 bearing acetyl substitutions on the FA moiety^a

Level of fragmentation energy, peptide sequence or fragment obtained	Value when X, Y, and FA are as indicated														
	X, Ala; Y, Thr; FA, C ₁₆			X, Gly; Y, Thr; FA, C ₁₈			X, Ala; Y, Val; FA, C ₁₈			X, Ala; Y, Val; FA, C ₁₈					
	m/z	Δ(ppm)	Sum formula	m/z	Δ(ppm)	Sum formula	m/z	Δ(ppm)	Sum formula	m/z	Δ(ppm)	Sum formula			
Low fragmentation energy (60 eV)															
[M+H] ⁺	1,265.7338	+0.7	C ₅₉ H ₁₀₃ N ₁₂ O ₁₈	1,279.7496	+0.9	C ₆₀ H ₁₀₃ N ₁₂ O ₁₈	1,293.7654	+0.8	C ₆₁ H ₁₀₅ N ₁₂ O ₁₇	1,277.7695	+1.6	C ₆₁ H ₁₀₅ N ₁₂ O ₁₇	1,291.7870	+0.1	C ₆₂ H ₁₀₇ N ₁₂ O ₁₇
[M-CH ₃ OH] ⁺	1,233.7170	-6.6	C ₅₈ H ₉₇ N ₁₂ O ₁₇	1,247.7194	+4.1	C ₅₉ H ₉₉ N ₁₂ O ₁₇	1,261.7494	-7.3	C ₆₀ H ₁₀₁ N ₁₂ O ₁₆	Low int.		C ₆₀ H ₁₀₁ N ₁₂ O ₁₆	Low int.		C ₆₁ H ₁₀₃ N ₁₂ O ₁₆
[M-CH ₃ OH-WMeAsn] ⁺	1,105.6558	-4.9	C ₅₃ H ₈₉ N ₁₀ O ₁₅	1,119.6619	+3.7	C ₅₄ H ₉₁ N ₁₀ O ₁₅	1,133.681	+0.6	C ₅₅ H ₉₃ N ₁₀ O ₁₄	1,117.6924	-5.0	C ₅₅ H ₉₃ N ₁₀ O ₁₄	1,131.7307	-25.0	C ₅₆ H ₉₅ N ₁₀ O ₁₄
[M-CH ₃ OH-WMeAsn-Dhb] ⁺	1,022.6180	-4.7	C ₄₉ H ₈₄ N ₉ O ₁₄	1,036.6365	-7.3	C ₅₀ H ₈₆ N ₉ O ₁₄	1,050.6478	-3.1	C ₅₁ H ₈₈ N ₉ O ₁₄	1,134.6603	-10.3	C ₅₁ H ₈₈ N ₉ O ₁₃	1,048.6671	-1.7	C ₅₂ H ₉₀ N ₉ O ₁₃
[M-CH ₃ OH-WMeAsn-Dhb-X] ⁺	951.5785	-2.5	C ₄₈ H ₈₃ N ₈ O ₁₃	979.589	+18.8	C ₄₈ H ₈₃ N ₈ O ₁₃	979.6041	+3.4	C ₄₈ H ₈₃ N ₈ O ₁₃	977.6481	-20.5	C ₄₉ H ₈₅ N ₈ O ₁₂	977.6518	-24.1	C ₄₉ H ₈₅ N ₈ O ₁₂
[M-CH ₃ OH-WMeAsn-Dhb-X-Gln] ⁺	823.5253	-9.4	C ₄₁ H ₇₁ N ₆ O ₁₁	851.5473	+1.8	C ₄₃ H ₇₅ N ₆ O ₁₁	851.5478	+1.2	C ₄₃ H ₇₅ N ₆ O ₁₁	849.5838	-16.7	C ₄₄ H ₇₆ N ₆ O ₁₀	849.5589	+12.5	C ₄₄ H ₇₇ N ₆ O ₁₀
[M-CH ₃ OH-WMeAsn-Dhb-X-Gln-Y] ⁺	722.4729	-4.2	C ₃₇ H ₆₄ N ₅ O ₉	750.5005	+0.9	C ₃₉ H ₆₈ N ₅ O ₉	750.5147	-18.1	C ₃₉ H ₆₈ N ₅ O ₉	Low int.		C ₄₀ H ₇₂ N ₅ O ₈	Low int.		C ₄₀ H ₇₂ N ₅ O ₈
[M-CH ₃ OH-WMeAsn-Dhb-X-Gln-Y-Thr] ⁺	621.4223	-0.2	C ₃₃ H ₅₇ N ₄ O ₇	649.4526	+1.4	C ₃₅ H ₆₁ N ₄ O ₇	649.4539	-0.6	C ₃₅ H ₆₁ N ₄ O ₇	649.465	-17.8	C ₃₃ H ₆₁ N ₄ O ₇	649.4483	+8.0	C ₃₅ H ₆₁ N ₄ O ₇
High fragmentation energy (100 eV)															
Fragment 1	411.3208	+2.2	C ₂₃ H ₄₃ N ₂ O ₄	439.3559	-6.5	C ₂₅ H ₄₇ N ₂ O ₄	439.3556	-5.8	C ₂₅ H ₄₇ N ₂ O ₄	439.3556	-5.8	C ₂₅ H ₄₇ N ₂ O ₄	439.3508	+5.1	C ₂₅ H ₄₇ N ₂ O ₄
Fragment 1, C ₂ H ₄ O ₂	351.3006	+0.0	C ₂₁ H ₃₉ N ₂ O ₂	379.3334	-4.0	C ₂₃ H ₄₃ N ₂ O ₂	379.3329	-2.6	C ₂₃ H ₄₃ N ₂ O ₂	379.3328	-2.4	C ₂₃ H ₄₃ N ₂ O ₂	379.3360	-10.8	C ₂₃ H ₄₃ N ₂ O ₂
Fragment 2	284.2583	+0.4	C ₁₇ H ₃₄ NO ₂	312.2919	-6.9	C ₁₉ H ₃₈ NO ₂	312.2892	+1.6	C ₁₉ H ₃₈ NO ₂	Low int.		C ₁₉ H ₃₈ NO ₂	Low int.		C ₁₉ H ₃₈ NO ₂
Fragment 2, C ₃ H ₄ O ₂	224.2367	+2.6	C ₁₅ H ₃₀ N	252.2686	0.0	C ₁₇ H ₃₄ N	252.2687	-0.5	C ₁₇ H ₃₄ N	252.2684	+0.7	C ₁₇ H ₃₄ N	252.2677	+3.5	C ₁₇ H ₃₄ N

^aLow int., low intensity (defined here as a signal-to-noise ratio lower than 2). For detailed methods, see Materials and Methods.

Downloaded from <http://aem.asm.org/> on February 19, 2019 by guest

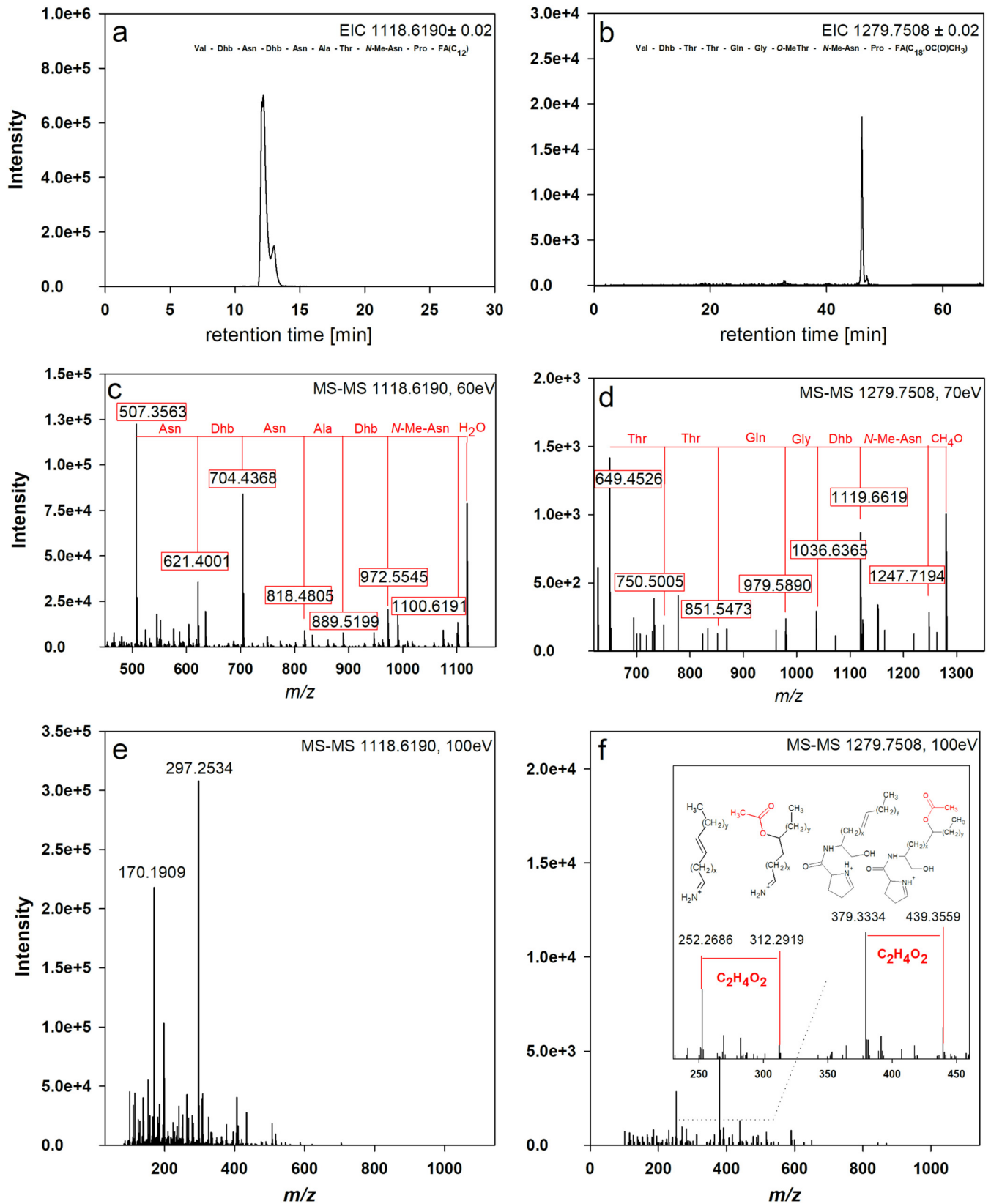


FIG 7 MS-MS fragmentation of MIN A (a, c, e) and the PUW variant at m/z 1,279 bearing an acetyl substitution of the fatty acid chain (b, d, f). (a, b) Base peak chromatograms. (c, d) Fragmentation of the protonated molecule at low fragmentation energy, yielding b series of ions, corresponding to the losses of particular amino acid residues. (e, f) Fragmentation of the protonated molecule at high energy (100 eV), yielding fragments characteristic for the β -amino fatty acid.

TABLE 4 Bacterial and yeast strains used for antimicrobial testing of PUW F and MIN A, C, and D

Test organism (HAMBI no.) ^a	Medium ^b	Incubation temp (°C)	Incubation time (h)	Gram stain reaction ^c
<i>Pseudomonas</i> sp. (2796)	TGY	28	24	–
<i>Micrococcus luteus</i> (2688)	TGY	28	24	+
<i>Bacillus subtilis</i> (251)	TGY	28	24	+
<i>Pseudomonas aeruginosa</i> (25)	TGY	37	24	–
<i>Escherichia coli</i> (396)	TGY	37	24	–
<i>Bacillus cereus</i> (1881)	TSA	28	24	+
<i>Burkholderia cepacia</i> (2487)	TSA	37	24	–
<i>Staphylococcus aureus</i> (11)	TSA	37	24	+
<i>Xanthomonas campestris</i> (104)	NA	28	24	–
<i>Burkholderia pseudomallei</i> (33)	NA	37	24	–
<i>Salmonella enterica</i> serovar Typhi (1306)	NA	37	24	–
<i>Arthrobacter globiformis</i> (1863)	NA	28	24	–
<i>Kocuria varians</i> (40)	NA	28	24	+
<i>Candida albicans</i> (261)	YM agar	37	24	Yeast
<i>Cryptococcus albidus</i> (264)	YM agar	28	24	Yeast
<i>Saccharomyces cerevisiae</i> (1164)	YM agar	28	24	Yeast

^aHAMBI, culture collection of University of Helsinki, Faculty of Agriculture and Forestry, Department of Microbiology.

^bThe compositions of all media were obtained from the American Type Culture Collection (ATCC). TGY, tryptone glucose yeast; TSA, tryptic soy agar; NA, nutrient agar; YM agar, yeast malt agar.

^c–, negative; +, positive.

Antimicrobial activity. Both PUWs and MINs possess cytotoxic activity against human cells *in vitro* (5, 10, 11). In the current study, we demonstrated that the major PUW/MIN variants (PUW F and MIN A, C, and D) did not exert antibacterial effects against either Gram-positive or Gram-negative bacteria in a panel of 13 selected strains (Table 4). PUW F was the only variant tested that manifested antagonistic activity against two yeast strains utilized in our experiment, namely, *Candida albicans* strain HAMBI 261 and *Saccharomyces cerevisiae* strain HAMBI 1164, with inhibition zones of 14 and 18 mm, respectively, and MICs of 6.3 $\mu\text{g ml}^{-1}$ (5.5 μM) (Fig. 8). No antifungal activity was recorded for the MIN C and D variants, and only weak inhibition of the two yeast strains was recorded for MIN A (Fig. S7). PUW F differs only slightly from MIN A, by a $-\text{CH}_2-\text{CH}_3$ extension of the FA moiety, indicating that the FA length affects bioactivity. Furthermore, the lack of bioactivity for MIN C and MIN D suggests that hydroxy and oxo substitutions also compromise antifungal efficacy. As previously demonstrated, cytotoxicity is due to membrane permeabilization activity accompanied by calcium flux into the cytoplasm (5), consistent with the membrane effects documented for other bacterial lipopeptides (4). However, as is apparent from our data (Fig. 8), PUW/MIN products appear to be effective solely against eukaryotes (thus far tested only on human and yeast cells). This finding is in contrast to the typical antibacterial activity frequently described for many lipopeptides produced by Gram-positive bacteria (4). Analogously, the cyanobacterial lipopeptides anabaenolysin A and hassalidins

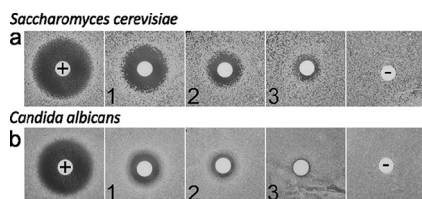


FIG 8 Antifungal activities of PUW F against yeast strains *Saccharomyces cerevisiae* HAMBI 1164 (a) and *Candida albicans* HAMBI 261 (b). Discs were treated with a range of concentrations from 25.2 $\mu\text{g ml}^{-1}$ to 0.0394 $\mu\text{g/ml}$ to determine the MIC. Numbers and symbols represent concentrations and controls, as follows: 1, 25.2 $\mu\text{g ml}^{-1}$; 2, 12.6 $\mu\text{g ml}^{-1}$; 3, 6.3 $\mu\text{g ml}^{-1}$; +, positive control (10 μg nystatin); –, negative control (10 μl methanol).

preferentially interact with cholesterol-containing membranes, hence their predisposition for activity against eukaryotic cells (6, 8).

Distribution of PUWs and MINs in cyanobacteria. PUWs and MINs form one of the most frequently reported groups of lipopeptides in cyanobacteria and have been isolated from heterocytous cyanobacteria, particularly members of the genera *Anabaena* and *Cylindrospermum* that inhabit soil (5, 9–11). Only a single study has mentioned the probable occurrence of puwainaphycins in a planktonic cyanobacterium (*Sphaerospermopsis*) (39). Our current comprehensive analysis of these lipopeptides and their biosynthetic genes further supports the hypothesis that lipopeptides occur predominantly in nonplanktonic biofilm-forming cyanobacteria (23). In this context, it is worth mentioning that *S. muelleri* strain 6 was isolated from a wetland bog in alpine mountains in coastal Norway (40). This strain is a toxigenic member of a biofilm microbiome and suspected to play a role in the development of severe hemolytic Alveld disease among outfield grazing sheep (41, 42). Biomass harvested from pure cultures of this strain exhibited strong cytotoxic activity toward primary rat hepatocytes (43, 44), which indicates the production of secondary metabolites with cytotoxic properties. Thus, the possible toxic potential of cyanobacterial lipopeptides, such as PUWs and MINs, in the environment warrants further attention.

Conclusions. Our study highlights and explores the extensive structural versatility of cyanobacterial lipopeptides from the PUW/MIN family by introducing previously unknown variants and newly sequenced biosynthetic gene clusters. Intriguingly, all variants are synthesized by a relatively conserved PKS/NRPS machinery with a common genetic origin. We hypothesize that chemical diversity is generated largely by the presence of two alternative fatty acyl-AMP ligase starter units, one of which exhibits an unusually broad specificity for FA substrates of various lengths. Additionally, putative halogenase and *O*-acetyltransferase genes were present in some gene clusters. This knowledge provides novel insight into the genetic background underpinning the biosynthesis of bacterial lipopeptides. The proposed biosynthetic mechanisms allow the studied microbes to generate a large pool of products that can be readily expanded by introducing relatively small genetic changes. This is consistent with the so-called “screening hypothesis” (45, 46), which predicts an evolutionary benefit for organisms producing a large chemical diversity of secondary metabolites at minimum cost. Accessory antimicrobial tests on bacteria and yeasts, together with previously published results, suggest a specific toxic effect of PUWs against eukaryotic cells. Thus, their toxic potential for humans and other animals clearly warrants further investigation, and their possible use as antifungal agents is ripe for exploration.

MATERIALS AND METHODS

Cultivation of cyanobacterial strains. Six cyanobacterial strains were included in the present study, *Cylindrospermum moravicum* CCALA 993 (strain 1), *Cylindrospermum alatosporum* CCALA 994 (strain 2), *Cylindrospermum alatosporum* CCALA 988 (strain 3), *Anabaena* sp. strain UHCC-0399 (previously *Anabaena* sp. strain SMIX 1; strain 4), *Anabaena minutissima* UTEX B 1613 (strain 5), and *Symplocastrum muelleri* NIVA-CYA 644 (strain 6). The origins of the strains are listed in Table 1. For chemical analysis, strains 1 to 5 were cultivated in BG-11 medium (47) in glass columns (300 ml) bubbled with air enriched in 1.5% CO₂ at a temperature of 28°C and constant illumination of 100 μmol photons m⁻² s⁻¹. Strain 6 was maintained in culture using a custom liquid medium obtained by mixing 200 ml of Z8 medium (48), 800 ml distilled water, 30 ml soil extract, and common vitamin premix (according to SAG [Sammlung von Algenkulturen der Universität Göttingen], but without biotin). Cultivation was performed in 100- to 200-ml Erlenmeyer flasks at 20°C with a 16:8 light/dark photoperiod under static conditions. Cultures were kept at low irradiance (4 μmol m⁻² s⁻¹ of photosynthetically active radiation [PhAR], generated using red-green-blue light-emitting-diode [RGB LED] strips). Cells were harvested by centrifugation (3,125 × *g*), stored at -80°C, and subsequently lyophilized. Strain 4 was cultivated at a larger scale for purification of major lipopeptide variants in a 10-liter tubular photobioreactor under the above-mentioned conditions in BG-11 medium.

Molecular and bioinformatic analyses. Single filaments of strains 2, 3, 5, and 6 were isolated for whole-genome amplification (WGA) and subsequent preparation of a whole-genome sequencing (WGS) library as described previously (12). Briefly, the glass capillary technique was used to isolate filaments and exclude minor bacterial contaminants. A set of 20 filaments from each strain was then used as a template for WGA. Multiple displacement amplification (MDA) using a Repli-g minikit (Qiagen, Hilden, Germany) was followed by PCR and sequencing to monitor the cyanobacterial 16S rRNA gene using primers 16S387F and 16S1494R (49). Positive samples (7 to 10 MDA products yielding clear 16S rRNA gene

sequences of the respective genera) were then pooled to create a template for WGS. DNA samples were sent for commercial *de novo* genome sequencing (EMBL Genomics Core Facility, Heidelberg, Germany) using the Illumina MiSeq platform (Illumina, San Diego, CA, USA) with an ~350-bp average-insert-length paired-end library and 250-bp reads (~1.4-Gbp data yield per strain). Raw data from *de novo* WGS were assembled using CLC Bio Genomics Workbench version 7.5 (CLC Bio, Aarhus, Denmark). Genomic DNA was isolated from strain 4 as previously described (37), and the quality was assessed using a NanoDrop 1000 spectrophotometer (Thermo Fisher Scientific, Waltham, MA, USA) and an Agilent TapeStation (Agilent Technologies, Santa Clara, CA, USA). High-molecular-weight DNA was used to construct an Illumina TruSeq PCR-free 350-bp library and sequenced using an Illumina HiSeq 2500 platform with a paired-end 100-cycle run. Genome data (1 Gb for each strain) were first checked using SPAdes version 3.7.1 (50) for read correction and removal of erroneous reads and then assembled using Newbler version 3.0 (454 Life Sciences, Branford, CT, USA). Genomic scaffolds were loaded into Geneious pro R10 (Biomatters) and investigated for FAAL and NRPS genes using BLASTp searches to identify putative lipopeptide synthetase gene clusters (23). FAAL and NRPS adenylation domains (A domains) from the single known PUW gene cluster (strain 1; [KM078884](#)) were used as queries since homologous gene clusters were expected. Contigs yielding high-similarity hits (E value of $<10^{-20}$) were then analyzed using the Glimmer 3 (51) algorithm to discover putative open-reading frames (ORFs). Functional annotation of ORFs was conducted by applying a combination of BLASTp/CDD searches against the NCBI database and using the antiSMASH 4.0 secondary metabolite gene cluster annotation pipeline (52, 53). Pairwise sequence identities and the presence of conserved residues in homologous putative proteins encoded in the gene clusters were assessed using Geneious pro software based on amino acid alignment (MAFFT plugin, default parameters). Minor assembly gaps were identified in the genomic scaffolds of all strains investigated, either directly after paired-end read assembly or based on mapping to the reference gene cluster from *C. alatosporum* CCALA 988. Gaps in PUW/MIN gene clusters were closed by PCR, and subsequent Sanger sequencing of PCR products was performed using custom primer annealing to regions adjacent to the assembly gaps.

Extraction and analysis of PUWs/MINs. To obtain comparable results, each strain was extracted using an identical ratio of lyophilized biomass (200 mg) to extraction solvent (10 ml of 70% methanol [MeOH], vol/vol). Extracts were evaporated using a rotary vacuum evaporator at 35°C and concentrated to 1 ml of 70% MeOH. The methanolic extracts were analyzed using a Thermo Scientific Dionex UltiMate 3000 ultra-high-performance liquid chromatography plus (UHPLC+) instrument equipped with a diode array detector connected to a Bruker Impact HD (Bruker, Billerica, MA, USA) high-resolution mass spectrometer with electrospray ionization. Separation of extracts was performed on a reversed-phase Phenomenex Kinetex C₁₈ column (150 by 4.6 mm, 2.6 μm) using H₂O (A)-acetonitrile (B) containing 0.1% HCOOH as a mobile phase, at a flow rate of 0.6 ml min⁻¹. The gradient was as follows: A/B 85/15 (0 min), 85/15 (over 1 min), 0/100 (over 20 min), 0/100 (over 25 min), and 85/15 (over 30 min). For better resolution of minor PUW variants, another analytical method with a longer gradient (67 min) adopted from our previous study (13) was applied. The peptide sequence was reconstructed from the *b* ion series obtained after opening of the ring between the proline and *N*-methylasparagine residues, followed by the sequential loss of water and all the amino acids with exception of the last residue (Pro). The numbers of carbons in the FA moiety in PUW/MIN variants containing nonsubstituted and hydroxy-/chloro-substituted FA were determined using a method described previously by our team (13). Characteristic FA immonium fragments in oxo-substituted PUW/MIN variants were identified by applying this method to crude extracts of *Anabaena* strain 5 containing the oxo-substituted MIN D variant (10). Since a stable, prominent, and characteristic FA immonium fragment with the sum formula C₁₅H₃₀NO⁺ was obtained for MIN D (Fig. S1), analogous fragments with the general formula C_xH_{2x}NO⁺ were used to identify oxo-substituted components in unknown PUW/MIN variants from other strains investigated.

Molecular networking. A molecular network was created using the Global Natural Products Social Molecular Networking (GNPS) online workflow (54). Data were filtered by removing all MS-MS peaks within ±17 Da of the precursor *m/z*. MS-MS spectra were window filtered by choosing only the top six peaks in the ±50-Da window throughout the spectrum. Data were then clustered with MS-Cluster with a parent mass tolerance of 0.1 Da and an MS-MS fragment ion tolerance of 0.025 Da to create consensus spectra. Additionally, consensus spectra comprised of fewer than two spectra were discarded. A network was then created in which edges were filtered using a cosine score above 0.75 and more than three matched peaks. Additional edges between pairs of nodes were retained in the network only when both nodes were included in each other's respective top 10 most similar nodes. Spectra in the network were then searched against the GNPS spectral libraries, and library spectra were filtered in the same manner as the input data. All matches obtained between network spectra and library spectra were retained only when the score was above 0.7 and at least four peaks matched. Analog searching was performed against the library with a maximum mass shift of 200 Da.

Purification of MINs from *Anabaena* sp. strain 4 and its NMR analysis. Freeze-dried biomass of strain 4 (10 g) was extracted with 70% MeOH (500 ml). The extract was evaporated using a rotary vacuum evaporator to reduce the MeOH content, and the sample was subsequently diluted with distilled water to reach a final MeOH concentration of >5%. The diluted extract was prepurified using a Supelco C₁₈ SPE cartridge (10 g, 60 ml) preequilibrated with 60 ml of MeOH and 120 ml of H₂O. After loading, retained components were eluted with 60 ml of pure MeOH, concentrated to dryness, and resuspended in 10 ml of pure MeOH. MIN A, C, and D were purified in two HPLC purification steps. The first step was performed on a preparative chromatographic system (Agilent 1260 Infinity series) equipped with a multiwavelength detector and automatic fraction collector. A preparative Reprosil 100 C₁₈ column (252 by 25 mm) was employed for separation at a flow rate of 10 ml min⁻¹ using the following gradient

of MeOH containing 0.1% HCOOH (A) and 10% MeOH containing 0.1% HCOOH (B): 0 min (100% B), 6 min (100% B), 15 min (43% B), 43 min (12% B), 45 min (0% B), 58 min (0% B), 60 min (100% B), and 64 min (100% B). Fractions were collected using an automatic fraction collector at 1-min intervals, and fractions were analyzed for MIN A, C, and D using the method described above. Fractions containing MIN A, C, and D were collected in separate vials and concentrated using a rotary evaporator. The second purification step was performed on a semipreparative HPLC (Agilent 1100 Infinity series) using a Reprosil 100 Phenyl column (250 by 8 mm) with acetonitrile containing 0.1% HCOOH (A) and water containing 0.1% HCOOH (B) using the following gradient: 0 min (60% B), 2 min (60% B), 6 min (50% B), 28 min (18% B), 30 min (0% B), 30 min (0% B), 32 min (0% B), 31 min (60% B), and 36 min (60% B). The flow rate was 1 ml min⁻¹ throughout, fractions were collected manually, and the purity was analyzed using the HPLC-HRMS method described above. NMR spectra of minutissamides were measured in dimethyl sulfoxide (DMSO)-*d*₆ at 30°C. All NMR spectra were collected using a Bruker Avance III 500 MHz NMR spectrometer, equipped with a 5-mm-diameter broadband probe (BBI) head with actively shielded z gradient.

Antibacterial and antifungal assays. The antimicrobial activities of four major variants (PUW F and MIN A, C, and D) were tested against 13 bacterial and two yeast strains (Table 4) using disc diffusion assays (8) in three independent experiments with kanamycin/nystatin and MeOH as positive and negative controls, respectively. The antifungal activity of PUW F was further evaluated by determining the MICs against *Candida albicans* (HAMBI 261) and *Saccharomyces cerevisiae* (HAMBI 1164) as described previously (8). PUW F was isolated from *Cylindrospermum* strain 1 according to a protocol described previously (5), and isolation of MIN A, C, and D was performed as described above. The variants produced by *S. muelleri* strain 6 were impossible to isolate due to the slow growth of the cyanobacterium, which resulted in low biomass yields during the study period.

Accession number(s). The accession numbers for the newly sequenced complete putative biosynthetic gene clusters uploaded to the European Nucleotide Archive are [MH325197](https://doi.org/10.1093/nucleotide/MH325197) to [MH325201](https://doi.org/10.1093/nucleotide/MH325201).

SUPPLEMENTAL MATERIAL

Supplemental material for this article may be found at <https://doi.org/10.1128/AEM.02675-18>.

SUPPLEMENTAL FILE 1, PDF file, 4.8 MB.

ACKNOWLEDGMENTS

This work was supported by Czech Science Foundation grant no. 16-09381S (Bioactive cyanobacterial lipopeptides: genome mining, detection, and structure-activity relationships), and by the Ministry of Education, Youth and Sports of the Czech Republic, National Program of Sustainability I, ID: LO1416 project ALGAMIC (ID: CZ.1.05/2.1.00/19.0392) and MSCA IF II project (CZ.02.2.69/0.0/0.0/18_070/0010493) as well as by Ministry of Regional Development of the Czech Republic—Cross-Border cooperation Czech-Bavaria project no. 41. Student participation (A. Kust and T. Galica) in the project was supported by The Grant Agency of the Faculty of Science, University of South Bohemia, grant GAJU 158/2016/P. Access to instruments and other facilities was supported by the Czech Research Infrastructure for Systems Biology (C4SYS; project no. LM2015055). This research was also supported by a grant from the NordForsk NCoE program NordAqua (project no. 82845) and by the Jane and Aatos Erkkö Foundation (K. Sivonen and J. Jokela), which mostly supported the structural elucidation of PUW variants. The Norwegian participation was supported by grants from the Department of Agriculture and Forestry, the County Governor of Møre og Romsdal, the County Governor of Sogn og Fjordane, the University of Oslo, and the Norwegian Institute for Water Research.

The authors declare no conflict of interest.

The funders had no role in study design, data collection and interpretation, or the decision to submit the work for publication.

REFERENCES

- Cochrane SA, Vederas JC. 2016. Lipopeptides from *Bacillus* and *Paenibacillus* spp.: a gold mine of antibiotic candidates. *Med Res Rev* 36:4–31. <https://doi.org/10.1002/med.21321>.
- Taylor SD, Palmer M. 2016. The action mechanism of daptomycin. *Bioorg Med Chem* 24:6253–6268. <https://doi.org/10.1016/j.bmc.2016.05.052>.
- Velkov T, Roberts KD, Li J. 2017. Rediscovering the octapeptins. *Nat Prod Rep* 34:295–309. <https://doi.org/10.1039/c6np00113k>.
- Ines M, Dhouha G. 2015. Lipopeptide surfactants: production, recovery and pore forming capacity. *Peptides* 71:100–112. <https://doi.org/10.1016/j.peptides.2015.07.006>.
- Hrouzek P, Kuzma M, Černý J, Novák P, Fišer R, Šimek P, Lukešová A, Kopecký J. 2012. The cyanobacterial cyclic lipopeptides puwainaphycins F/G are inducing necrosis via cell membrane permeabilization and subsequent unusual actin relocalization. *Chem Res Toxicol* 25:1203–1211. <https://doi.org/10.1021/tx300044t>.
- Oftedal L, Myhren L, Jokela J, Gausdal G, Sivonen K, Doskeland SO, Herfindal L. 2012. The lipopeptide toxins anabaenolysin A and B target biological membranes in a cholesterol-dependent manner. *Biochim Biophys Acta Biomembr* 1818:3000–3009. <https://doi.org/10.1016/j.bbamem.2012.07.015>.
- Tomek P, Hrouzek P, Kuzma M, Sýkora J, Fišer R, Černý J, Novák P, Bártová S, Šimek P, Hof M, Kavan D, Kopecký J. 2015. Cytotoxic

- lipopeptide muscovotoxin A, isolated from soil cyanobacterium *Desmonostoc muscorum*, permeabilizes phospholipid membranes by reducing their fluidity. *Chem Res Toxicol* 28:216–224. <https://doi.org/10.1021/tx500382b>.
8. Vestola J, Shishido TK, Jokela J, Fewer DP, Aitio O, Permi P, Wahlsten M, Wang H, Rouhiainen L, Sivonen K. 2014. Hassallidins, antifungal glycolipopeptides, are widespread among cyanobacteria and are the end-product of a nonribosomal pathway. *Proc Natl Acad Sci U S A* 111: E1909–E1917. <https://doi.org/10.1073/pnas.1320913111>.
 9. Gregson JM, Chen JL, Patterson GML, Moore RE. 1992. Structures of puwainaphycins A-E. *Tetrahedron* 48:3727–3734. [https://doi.org/10.1016/S0040-4020\(01\)92264-1](https://doi.org/10.1016/S0040-4020(01)92264-1).
 10. Kang HS, Kronic A, Shen Q, Swanson SM, Orjala J. 2011. Minutissamides A-D, antiproliferative cyclic decapeptides from the cultured cyanobacterium *Anabaena minutissima*. *J Nat Prod* 74:1597–1605. <https://doi.org/10.1021/jp2002226>.
 11. Kang HS, Sturdy M, Kronic A, Kim H, Shen Q, Swanson SM, Orjala J. 2012. Minutissamides E-L, antiproliferative cyclic lipodecapeptides from the cultured freshwater cyanobacterium cf. *Anabaena* sp. *Bioorg Med Chem* 20:6134–6143. <https://doi.org/10.1016/j.bmc.2012.08.017>.
 12. Mareš J, Hájek J, Urajová P, Kopecký J, Hrouzek P. 2014. A hybrid non-ribosomal peptide/polyketide synthetase containing fatty-acyl ligase (FAAL) synthesizes the beta-amino fatty acid lipopeptides puwainaphycins in the cyanobacterium *Cylindrospermum alatosporum*. *PLoS One* 9:e111904. <https://doi.org/10.1371/journal.pone.0111904>.
 13. Urajová P, Hájek J, Wahlsten M, Jokela J, Galica T, Fewer DP, Kust A, Zapomělová-Kozlíková E, Delawska K, Sivonen K, Kopecký J, Hrouzek P. 2016. A liquid chromatography-mass spectrometric method for the detection of cyclic beta-amino fatty acid lipopeptides. *J Chromatogr A* 1438:76–83. <https://doi.org/10.1016/j.chroma.2016.02.013>.
 14. Cheel J, Urajová P, Hájek J, Hrouzek P, Kuzma M, Bouju E, Faure K, Kopecký J. 2017. Separation of cyclic lipopeptide puwainaphycins from cyanobacteria by countercurrent chromatography combined with polymeric resins and HPLC. *Anal Bioanal Chem* 409:917–930. <https://doi.org/10.1007/s00216-016-0066-z>.
 15. Moore RE, Bornemann W, Niemczura WP, Gregson JM, Chen JL, Norton TR, Patterson GML, Helms GL. 1989. Puwainaphycin C, a cardioactive cyclic peptide from the blue-green alga *Anabaena* BQ-16-1. Use of two dimensional carbon-13-carbon-13 and carbon-13-nitrogen-15 correlation spectroscopy in sequencing the amino acid units. *J Am Chem Soc* 111:6128–6132. <https://doi.org/10.1021/ja00198a021>.
 16. Duitman EH, Hamoen LW, Rembold M, Venema G, Seitz H, Saenger W, Bernhard F, Reinhardt R, Schmidt M, Ullrich C, Stein T, Leenders F, Vater J. 1999. The mycosubtilin synthetase of *Bacillus subtilis* ATCC6633: a multifunctional hybrid between a peptide synthetase, an amino transferase, and a fatty acid synthase. *Proc Natl Acad Sci U S A* 96: 13294–13299. <https://doi.org/10.1073/pnas.96.23.13294>.
 17. Tsuge K, Akiyama T, Shoda M. 2001. Cloning, sequencing, and characterization of the iturin A operon. *J Bacteriol* 183:6265–6273. <https://doi.org/10.1128/JB.183.21.6265-6273.2001>.
 18. Koumoutsis A, Chen XH, Henne A, Liesegang H, Hitzeroth G, Franke P, Vater J, Borriss R. 2004. Structural and functional characterization of gene clusters directing nonribosomal synthesis of bioactive cyclic lipopeptides in *Bacillus amyloquelici* strain FZB42. *J Bacteriol* 186: 1084–1096. <https://doi.org/10.1128/JB.186.4.1084-1096.2004>.
 19. Sood S, Steinmetz H, Beims H, Mohr KI, Stadler M, Djukic M, von der Ohe W, Steinert M, Daniel R, Müller R. 2014. Paenilarvins: iturin family lipopeptides from the honey bee pathogen *Paenibacillus larvae*. *ChemBiochem* 15:1947–1955. <https://doi.org/10.1002/cbic.201402139>.
 20. Ramaswamy AV, Sorrels CM, Gerwick WH. 2007. Cloning and biochemical characterization of the hectochlorin biosynthetic gene cluster from the marine cyanobacterium *Lyngbya majuscula*. *J Nat Prod* 70: 1977–1986. <https://doi.org/10.1021/np0704250>.
 21. Micallef ML, D'Agostino PM, Sharma D, Viswanathan R, Moffitt MC. 2015. Genome mining for natural product biosynthetic gene clusters in the subsection V cyanobacteria. *BMC Genomics* 16:669. <https://doi.org/10.1186/s12864-015-1855-z>.
 22. Edwards DJ, Marquez BL, Nogle LM, McPhail K, Goeger DE, Roberts MA, Gerwick WH. 2004. Structure and biosynthesis of the jamaicamides, new mixed polyketide-peptide neurotoxins from the marine cyanobacterium *Lyngbya majuscula*. *Chem Biol* 11:817–833. <https://doi.org/10.1016/j.chembiol.2004.03.030>.
 23. Galica T, Hrouzek P, Mareš J. 2017. Genome mining reveals high incidence of putative lipopeptide biosynthesis NRPS/PKS clusters containing fatty acyl-AMP ligase genes in biofilm-forming cyanobacteria. *J Phycol* 53:985–998. <https://doi.org/10.1111/jpy.12555>.
 24. Arora P, Goyal A, Natarajan VT, Rajakumara E, Verma P, Gupta R, Yousef M, Trivedi OA, Mohanty D, Tyagi A, Sankaranarayanan R, Gokhale RS. 2009. Mechanistic and functional insights into fatty acid activation in *Mycobacterium tuberculosis*. *Nat Chem Biol* 5:166–173. <https://doi.org/10.1038/nchembio.143>.
 25. Liu Z, Ioeberger TR, Wang F, Sacchetti JC. 2013. Structures of *Mycobacterium tuberculosis* FadD10 protein reveal a new type of adenylate-forming enzyme. *J Biol Chem* 288:18473–18483. <https://doi.org/10.1074/jbc.M113.466912>.
 26. Coates RC, Podell S, Korobeynikov A, Lapidus A, Pevzner P, Sherman DH, Allen EE, Gerwick L, Gerwick WH. 2014. Characterization of cyanobacterial hydrocarbon composition and distribution of biosynthetic pathways. *PLoS One* 9:e85140. <https://doi.org/10.1371/journal.pone.0085140>.
 27. Mohanty D, Sankaranarayanan R, Gokhale RS. 2011. Fatty acyl-AMP ligases and polyketide synthases are unique enzymes of lipid biosynthetic machinery in *Mycobacterium tuberculosis*. *Tuberculosis (Edinb)* 91:448–455. <https://doi.org/10.1016/j.tube.2011.04.006>.
 28. Goyal A, Verma P, Anandhakrishnan M, Gokhale RS, Sankaranarayanan R. 2012. Molecular basis of the functional divergence of fatty acyl-AMP ligase biosynthetic enzymes of *Mycobacterium tuberculosis*. *J Mol Biol* 416:221–238. <https://doi.org/10.1016/j.jmb.2011.12.031>.
 29. Villiers BRM, Hollfelder F. 2009. Mapping the limits of substrate specificity of the adenylation domain of TycA. *Chembiochem* 10:671–682. <https://doi.org/10.1002/cbic.200800553>.
 30. Christiansen G, Philmus B, Hemscheidt T, Kurmayer R. 2011. Genetic variation of adenylation domains of the anabaenopeptin synthesis operon and evolution of substrate promiscuity. *J Bacteriol* 193: 3822–3831. <https://doi.org/10.1128/JB.00360-11>.
 31. Brandenburger E, Braga D, Kombrink A, Lackner G, Gressler J, Künzler M, Hoffmeister D. 2018. Multi-genome analysis identifies functional and phylogenetic diversity of basidiomycete adenylate-forming reductases. *Fungal Genet Biol* 112:55–63. <https://doi.org/10.1016/j.fgb.2016.07.008>.
 32. Rouhiainen L, Jokela J, Fewer DP, Urmann M, Sivonen K. 2010. Two alternative starter modules for the non-ribosomal biosynthesis of specific anabaenopeptin variants in *Anabaena* (Cyanobacteria). *Chem Biol* 17:265–273. <https://doi.org/10.1016/j.chembiol.2010.01.017>.
 33. Kleigrewe K, Almaliti J, Tian IY, Kinnel RB, Korobeynikov A, Monroe EA, Duggan BM, Di Marzo V, Sherman DH, Dorrestein PC, Gerwick L, Gerwick WH. 2015. Combining mass spectrometric metabolic profiling with genomic analysis: a powerful approach for discovering natural products from cyanobacteria. *J Nat Prod* 78:1671–1682. <https://doi.org/10.1021/acs.jnatprod.5b00301>.
 34. Voráčková K, Hájek J, Mareš J, Urajová P, Kuzma M, Cheel J, Villunger A, Kapuscik A, Bally M, Novák P, Kabeláč M, Krumschnabel G, Lukeš M, Voloshko L, Kopecký J, Hrouzek P. 2017. The cyanobacterial metabolite nocuolin A is a natural oxadiazine that triggers apoptosis in human cancer cells. *PLoS One* 12:e0172850. <https://doi.org/10.1371/journal.pone.0172850>.
 35. He J, Hertweck C. 2004. Biosynthetic origin of the rare nitroaryl moiety of the polyketide antibiotic aureothin: involvement of an unprecedented N-oxygenase. *J Am Chem Soc* 126:3694–3695. <https://doi.org/10.1021/ja039328t>.
 36. Choi YS, Zhang HJ, Brunzelle JS, Nair SK, Zhao HM. 2008. In vitro reconstitution and crystal structure of p-aminobenzoate N-oxygenase (AurF) involved in aureothin biosynthesis. *Proc Natl Acad Sci U S A* 105:6858–6863. <https://doi.org/10.1073/pnas.0712073105>.
 37. Fewer DP, Wahlsten M, Osterholm J, Jokela J, Rouhiainen L, Kaasalainen U, Rikkinen J, Sivonen K. 2013. The genetic basis for O-acetylation of the microcystin toxin in cyanobacteria. *Chem Biol* 20:861–869. <https://doi.org/10.1016/j.chembiol.2013.04.020>.
 38. Murray IA, Shaw WV. 1997. O-acetyltransferases for chloramphenicol and other natural products. *Antimicrob Agents Chemother* 41:1–6.
 39. Zapomělová E, Jezberová J, Hrouzek P, Hisem D, Řeháková K, Komárková J. 2009. Polyphasic characterization of three strains of *Anabaena reniformis* and *Aphanizomenon aphanizomenoides* (cyanobacteria) and their reclassification to *Sphaerospermum* gen. nov. (incl. *Anabaena kisseleviana*). *J Phycol* 45:1363–1373. <https://doi.org/10.1111/j.1529-8817.2009.00758.x>.
 40. Skulberg OM, Mysterud I, Karlsen J, Tønnesen HH, Laane CMM, Schumacher T. 2012. Alveld research per annum 2012: searchlight on cyanobacteria we have minor knowledge of. *Biolog* 30:32–41. (In Norwegian.)
 41. Tønnesen HH, Mysterud I, Karlsen J, Skulberg OM, Laane CMM, Schum-

- acher T. 2013. Identification of singlet oxygen photosensitizers in lambs drinking water in an alveld risk area in West Norway. *J Photochem Photobiol B* 119:37–45. <https://doi.org/10.1016/j.jphotobiol.2012.12.003>.
42. Hegge AB, Myrnes I, Karlsen J, Skulberg OM, Laane CMM, Schumacher T, Tønnesen HH. 2013. Impaired secondary oxidant deactivation capacity and enhanced oxidative stress in serum from alveld affected lambs. *J Photochem Photobiol B* 126:126–134. <https://doi.org/10.1016/j.jphotobiol.2013.07.005>.
43. Heinze R. 1996. A biotest for hepatotoxins using primary rat hepatocytes. *Phycologia* 35:89–93. <https://doi.org/10.2216/10031-8884-35-65-89.1>.
44. Skulberg OM. 1996. Toxins produced by cyanophytes in Norwegian inland waters—health and environment, p 197–216. In Låg J (ed), *Chemical data as a basis of geomedical investigations. The Norwegian Academy of Science and Letters, Oslo, Norway*.
45. Jones CG, Firn RD. 1991. On the evolution of plant secondary chemical diversity. *Philos Trans R Soc Lond B* 333:273–280. <https://doi.org/10.1098/rstb.1991.0077>.
46. Firn RD, Jones CG. 2000. The evolution of secondary metabolism: a unifying model. *Mol Microbiol* 37:989–994.
47. Rippka R, Deruelles J, Waterbury JB, Herdman M, Stanier RY. 1979. Generic assignments, strain histories and properties of pure cultures of cyanobacteria. *J Gen Microbiol* 111:1–61. <https://doi.org/10.1099/00221287-111-1-1>.
48. Skulberg R, Skulberg OM. 1990. Research with algal cultures—NIVA's Culture Collection of Algae. NIVA report. Norwegian Institute for Water Research, Oslo, Norway.
49. Taton A, Grubisic S, Brambilla E, De Wit R, Wilmotte A. 2003. Cyanobacterial diversity in natural and artificial microbial mats of Lake Fryxell (McMurdo dry valleys, Antarctica): a morphological and molecular approach. *Appl Environ Microbiol* 69:5157–5169. <https://doi.org/10.1128/AEM.69.9.5157-5169.2003>.
50. Bankevich A, Nurk S, Antipov D, Gurevich A, Dvorkin M, Kulikov AS, Lesin V, Nikolenko S, Pham S, Prjibelski A, Pyshkin A, Sirotkin A, Vyahhi N, Tesler G, Alekseyev MA, Pevzner PA. 2012. SPAdes: a new genome assembly algorithm and its applications to single-cell sequencing. *J Comput Biol* 19:455–497. <https://doi.org/10.1089/cmb.2012.0021>.
51. Delcher AL, Bratke KA, Powers EC, Salzberg SL. 2007. Identifying bacterial genes and endosymbiont DNA with Glimmer. *Bioinformatics* 23: 673–679. <https://doi.org/10.1093/bioinformatics/btm009>.
52. Weber T, Blin K, Duddela S, Krug D, Kim HU, Brucoleri R, Lee SY, Fischbach MA, Müller R, Wohlleben W, Breitling R, Takano E, Medema MH. 2015. antiSMASH 3.0—a comprehensive resource for the genome mining of biosynthetic gene clusters. *Nucleic Acids Res* 43:W237–W243. <https://doi.org/10.1093/nar/gkv437>.
53. Blin K, Wolf T, Chevrette MG, Lu XW, Schwalen CJ, Kautsar SA, Duran HGS, Santos E, Kim HU, Nave M, Dickschat JS, Mitchell DA, Shelest E, Breitling R, Takano E, Lee SY, Weber T, Medema MH. 2017. antiSMASH 4.0—improvements in chemistry prediction and gene cluster boundary identification. *Nucleic Acids Res* 45:W36–W41. <https://doi.org/10.1093/nar/gkx319>.
54. Wang M, Carver JJ, Phelan VV, Sanchez LM, Garg N, Peng Y, Nguyen DD, Watrous J, Kapono CA, Luzzatto-Knaan T, Porto C, Bouslimani A, Melnik AV, Meehan MJ, Liu W-T, Crüsemann M, Boudreau PD, Esquenazi E, Sandoval-Calderón M, Kersten RD, Pace LA, Quinn RA, Duncan KR, Hsu C-C, Floros DJ, Gavilan RG, Kleigrewe K, Northen T, Dutton RJ, Parrot D, Carlson EE, Aigle B, Michelsen CF, Jelsbak L, Sohlenkamp C, Pevzner P, Edlund A, McLean J, Piel J, Murphy BT, Gerwick L, Liaw C-C, Yang Y-L, Humpf H-U, Maansson M, Keyzers RA, Sims AC, et al. 2016. Sharing and community curation of mass spectrometry data with Global Natural Products Social Molecular Networking. *Nat Biotechnol* 34:828–837. <https://doi.org/10.1038/nbt.3597>.
55. Johansen JR, Bohunická M, Lukešová A, Hrčková K, Vaccarino MA, Chesarino NM. 2014. Morphological and molecular characterization within 26 strains of the genus *Cylindrospermum* (Nostocaceae, Cyanobacteria) with descriptions of three new species. *J Phycol* 50:187–202. <https://doi.org/10.1111/jpy.12150>.
56. Tamrakar A. 2016. Isolation of benthic cyanobacteria and screening of bioactivities and natural products from culture collection strains. Master's Thesis. University of Helsinki, Helsinki, Finland.
57. Kantz T, Bold HC. 1969. Phycological studies IX. Morphological and taxonomic investigations of *Nostoc* and *Anabaena* in culture. Publication no. 6924. University of Texas, Austin, TX.